Mixed-Potential-Type NO_x Sensor Based on YSZ and Zinc Oxide Sensing Electrode

N. Miura[1*], K. Akisada[1], J. Wang[1], S. Zhuiykov[1] and T. Ono[2]

[1]Art, Science and Technology Center for Cooperative Research,

Kyushu University, Kasuga-shi, Fukuoka 816-8580, Japan

[2] R&D Division, Riken Corporation, Kumagaya, Saitama 360-8522, Japan

Abstract. Electrochemical sensors using tubular yttria-stabilized zirconia (YSZ) and oxide sensing electrode (SE) were fabricated and examined for NO_x detection at high temperatures. The mixed-potential-type NO_x sensor using ZnO-SE gave the highest sensitivity to NO_x among other single-type oxides tested as SEs in the temperature range of 600-700 °C. The response of the ZnO-attached device was a linear for the logarithm of NO_2 (NO) concentrations from 40 to 450 ppm. The sensing mechanism of the sensor was discussed on the basis of the gas adsorption-desorption behavior, the catalytic activity data, and electrochemical behavior for oxides examined.

1. Introduction

One of the most desirable applications for *"in-situ"* solid electrolyte NO_x sensors is monitoring and controlling NO_x concentration in car exhausts. However, it is necessary to develop compact reliable NO_x sensors capable of operation at temperatures above ca. 600 °C to meet the requirements of automotive industry for such instruments. In addition, recent legislation in EU, Japan and USA has significantly increased demand for solid-state gas sensors. For example, the EU emission limits for passenger cars and heavy-duty diesel vehicles will be reconsidered soon again [1]. So far, the most reliable sensors in the very harsh high-temperature environment of car exhausts are YSZ-based oxygen sensors (λ-sensors). Their attractive features, such as low cost, fast response, and compactness, have led to their extensive use for on-line emission control, and their production for the world-wide automotive industry has been rising rapidly and already reached one hundred million pieces per year.

The automotive industry has released new ultra lean-burn (or direct-injection type) engine systems to improve fuel efficiency as well as to reduce CO_2 emissions from the engine system. In this ultra-lean-burn engine system, a new NO_x-storage catalyst is needed for compensation of the low NO_x-removal ability of the conventional three-way catalyst under lean-burn (air rich) condition. The NO_x concentration in the exhaust gas coming from the NO_x-storage catalyst increases gradually with time due to the saturation of NO_x-storage capacity of the catalyst as shown in Fig. 1 [2]. Fuel-rich gas containing high concentrations of hydrocarbons is allowed to flow through the catalyst to regenerate the storage ability. As a result, NO_x concentration in the gas emitted from this new catalyst decreases rapidly down to zero level and then gradually increases again. It is, therefore, important to install *"in-situ"* NO_x sensors to optimize the catalyst performance. One of the major requirements of the *on-board* NO_x sensor is determination of NO_x concentration in several-tens-ppm level in the downstream of new catalyst so that the timing for regenerating the catalyst can be adjusted.

Solid-state gas sensors based on mixed-potential have gained a great deal of interest in the scientific and

*Corresponding author. Tel: +81-92-583-8852; Fax: +81-92-583-8976, E-mail: miura@astec.kyushu-u.ac.jp

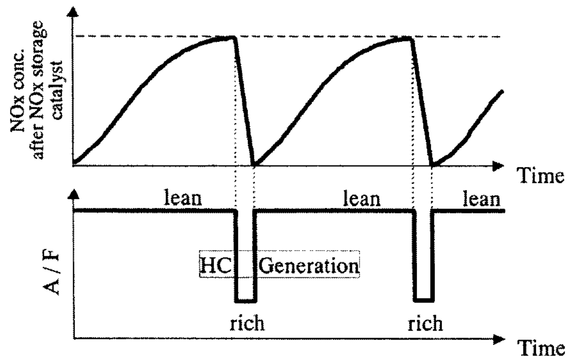

Fig. 1. Regeneration pattern of new NO_x-storage catalyst for a direct-injection-type engine.

technological sensor communities [3]. The special attention has been paid lately to the YSZ-based sensors using single-type and spinel-type oxide SEs due to their high sensing performances to various gaseous pollutants in oxygen containing atmospheres at high temperatures. Table 1 provides typical examples of characteristics of the mixed-potential type YSZ-based gas-sensing-devices using oxide SE reported by the authors to date. For instance, we have extensively investigated several oxides as SEs for NO_x sensing, such as $CdMn_2O_4$ [4], $CdCr_2O_4$ [5], WO_3 [6], $NiCr_2O_4$ [7], $ZnFe_2O_4$ [8] and $ZnCr_2O_4$ [9,10], since our first report in 1996 [3] suggested that the use of oxide SE in this type of NO_x sensor is very effective for sensitive detection of NO_2 at high temperatures. Several papers [14-18] dealing with oxides as a sensing electrode of mixed-potential-type NO_x sensor have also been published by several research groups after our first report in 1996. Specifically, we investigated the zinc-family oxides as SEs for NO_x sensors [8-10]. Consequently, we have found that, among the single-type oxides examined, the ZnO-SE is most stable and gives the highest sensitivity to NO_x at temperature as high as 700 °C. Therefore, in this study the main sensing properties of the YSZ-based mixed-potential NO_x sensor using ZnO-SE have been investigated.

2. Experimental Description

Commercial half-opened YSZ tubes (8 mol.% Y_2O_3 doped, NKT Co., Ltd.) were used for fabrication of NO_x sensors. The tubes were 300 mm in length and 5 and 8 mm in inner and outer diameter, respectively. Commercially available oxide powders were applied on the outer surface of the YSZ tube and then sintered at 1200 °C for 2 h to form the SE. The Pt paste was applied on the inner surface of the YSZ tube and then sintered at 1200 °C for 2 h to form the counter electrode (CE). The sensing performances were evaluated in a conventional gas-flow apparatus in the temperature range of 600-700 °C from 40 ppm up to 450 ppm of NO_x concentration. The ppm refers to the volume concentration of NO_x in the gaseous mixture. The flow rate of the sample gas (or base air) was fixed at 100 cm^3/min. The difference in potential (EMF) between SE and CE was measured by means of a digital electrometer (Advantest, R8240) as a sensing signal of the mixed-potential-type sensor when SE was exposed to the base air or to the sample gas with different NO_x concentrations. The CE was always exposed to the atmospheric air during the experiments.

Table 1. Typical examples of sensing characteristics of the mixed-potential YSZ-based devices using oxide-SE reported by us.

Gas	Oxide sensing electrode	Operating temperature (°C)	Measuring concentrations (ppm)	Year of publication	Reference number
NO_x	$CdMn_2O_4$	500 – 600	5 ~ 4000	1996	[3,4]
	$CdCr_2O_4$	500 – 600	20 ~ 600	1997	[5]
	WO_3	500 – 700	5 ~ 200	2000	[6]
	$NiCr_2O_4$	550 – 650	15 ~ 500	2001	[7]
	$ZnFe_2O_4$	550 – 700	20 ~ 500	2001	[8,9]
	$ZnCr_2O_4$	550 – 650	20 ~ 500	2002	[10]
CO	$CdO+SnO_2$	600	20 ~ 4000	1997	[11]
H_2S	Au - WO_3	400	0.6 ~ 50	1994	[12]
C_3H_6	CdO	600	30 ~ 800	2000	[13]

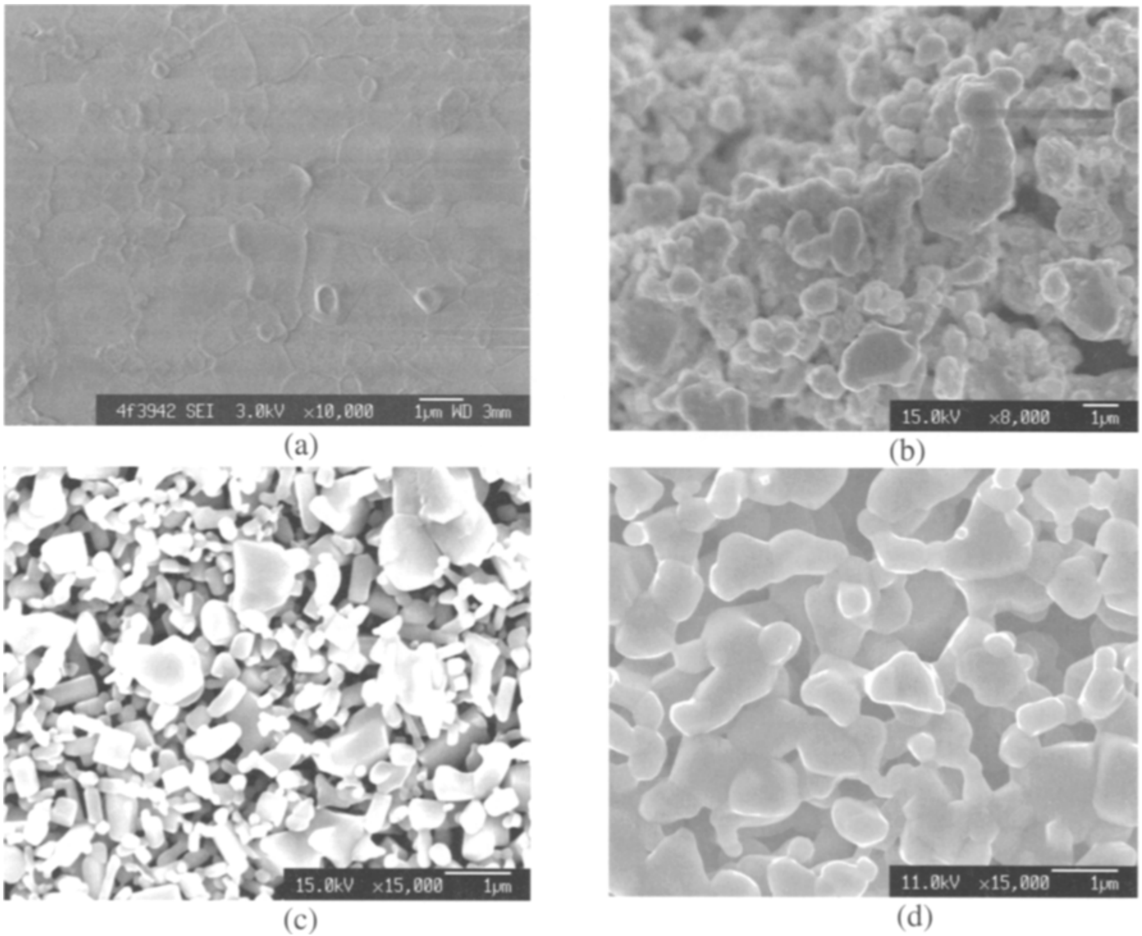

Fig. 2. SEM images of the surface of YSZ substrate (a), Pt electrode layer (b), ZnO layer sintered at 800 °C (c) and ZnO layer sintered at 1200 °C (d).

The crystal structure and the surface state of various sensor materials used here were investigated by means of XRD analysis (with CuKα radiation) and SEM observation. XRD measurements were carried out with a RIGAKU X-ray diffractometer (RINT 2100VLR/PC). SEM observation was performed by using JEOL electron microscope (JSM-6340F) operating at 3.0 kV or 15.0 kV. The adsorption-desorption behavior of NO_2 and O_2 were examined using a temperature-programmed desorption (TPD) apparatus (Bell Japan Inc., TPD-1-AT). The oxide powder (0.3 g) was set in the quartz-glass cell of the TPD apparatus. The sample was heated up to 800 °C in an He gas stream and was exposed to pure O_2 at this temperature, followed by cooling down to 50 °C in the O_2 stream. Then, the sample was treated with 1000 ppm NO_2 diluted with He at 50 °C for 5 min for the NO_2 adsorption. The desorbed NO_x and O_2 from the sample were detected with a chemiluminescence NO_x analyzer (Yanako, ECL-88A) and a QP-mass spectrometer, respectively, when the sample was heated up to 800 °C at heating rate of 10 °C/min in a He stream. The catalytic activity of each oxide (0.01 g) for the gas-phase decomposition of NO_2 was evaluated by using the TPD apparatus as well as the NO_x analyzer in the temperature range of 200-700 °C.

3. Results and Discussion

3.1. Crystal Structure and Surface State of Sensor Materials. All peaks in the XRD spectrum for ZnO annealed at 1200 °C could be assigned to ZnO (JCPDS 22-1010). Figure 2 shows SEM images of the surfaces of YSZ substrate *(a)*, Pt electrode *(b)*, ZnO layer sintered at 800 °C *(c)* and ZnO layer sintered at 1200 °C *(d)*. The surface of YSZ substrate has no open porosity and a grain is sized from 1 µm to 3 µm. The Pt electrode was porous with an average particle size of about 1 µm. The ZnO layer sintered at 800 °C was very porous with the average

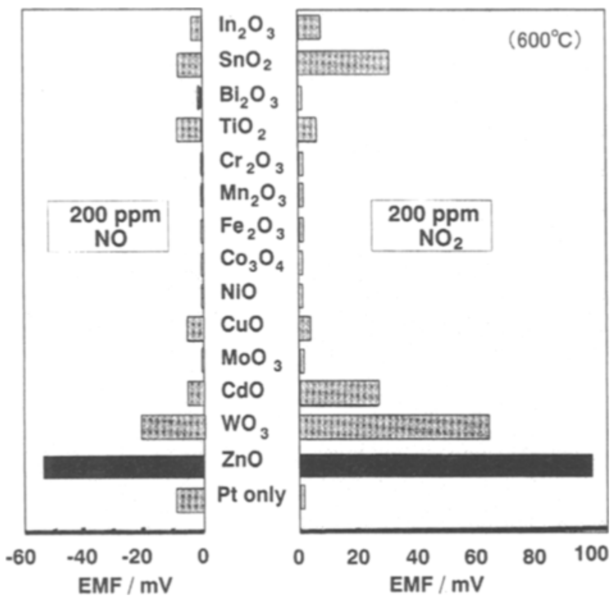

Fig. 3. EMF values at 600 °C to both NO and NO_2 (200 ppm each) in air for the tubular YSZ-based sensors using each of several single-oxide SEs tested.

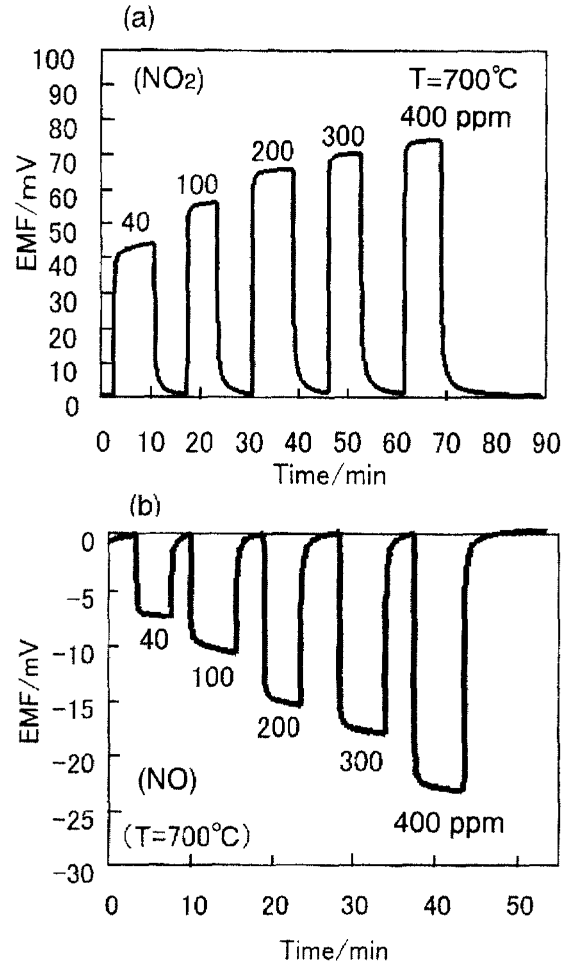

Fig. 5. Response transients to NO_2 (a) and NO (b) for the YSZ-based sensor using ZnO-SE at 700 °C.

grain size in the 0.2-0.6 μm range. However, sintering of the ZnO layer at 1200 °C provided larger grain sizes from 0.5 μm to 1 μm in average. This result suggests that the thermal treatment brings about the structural stability and the low surface-to-volume ratio for ZnO, which is very important for good sensing characteristics of the sensor.

3.2. Sensing Performances of the NO_x Sensor. The EMF in response to both NO and NO_2 concentrations (200 ppm each) in air for the tubular YSZ-based sensors using several single-oxide SEs tested at 600 °C are shown in Fig. 3. The EMF value was close to zero in the carrier gas (dry synthetic air), so the measured EMF values were considered as the sensitivities to NO and NO_2. As clearly shown in this figure, ZnO-SE gave the highest sensitivity to both NO and NO_2 among other single-oxides tested as SE. Figure 4 shows that the EMF response of the YSZ-based sensor using ZnO-SE depends linearly on the logarithm of NO_x concentration from 50 ppm up to 450 ppm in the tested temperature range of 600-700 °C. It is also evident that among the examined and previously published oxide SEs [3-10], ZnO gave one of the highest sensitivity to NO_2 in the above-mentioned temperature range: the EMF value of the present sensor to 50 ppm

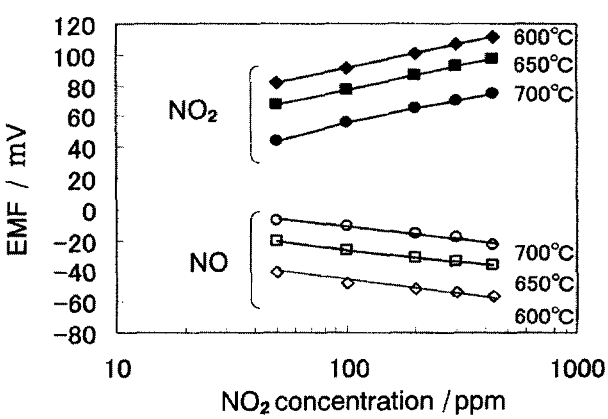

Fig. 4. NO_x sensing characteristics for the YSZ-based sensor using ZnO-SE in the tested temperature range of 600-700 °C.

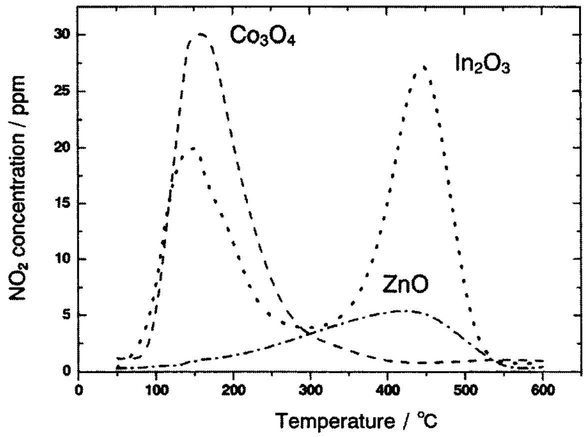

Fig. 6. TPD profiles of NO_2 from ZnO, In_2O_3 and Co_3O_4 powder samples.

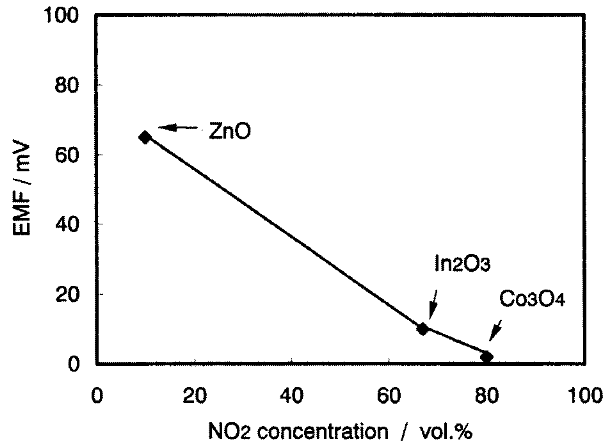

Fig. 8. Correlation between EMF value (NO_2 sensitivity) and NO_2 conversion for the three oxides tested.

NO_2 was as high as ca. 40 mV even at 700 °C. In addition, the evaluation of sensing performances of the NOx sensors using ZnO-SE showed that the NO_x sensitivities gave little degradation even at 700 °C during the test period of about one month. The response transients to different concentration of both NO_2 (a) and to NO (b) for the YSZ-based sensor using ZnO-SE at 700 °C are shown in Fig. 5. The 90% response time was within 60 s at 700 °C for all NO_x concentrations tested.

3.3. Examination of Sensing Mechanism. To understand the mechanism by which the ZnO-SE provides such a high NO_2 sensitivity at high temperatures, various properties of the representative oxides (ZnO, In_2O_3, Co_3O_4), such as gas adsorption-desorption behavior, oxygen sensing characteristics, and the catalytic activity for the gas-phase decomposition reaction of NO_2, have been examined.

The TPD profiles of NO_2 from ZnO, In_2O_3 and Co_3O_4 samples, shown in Fig. 6, reveal that the amount of NO_2 desorption from Co_3O_4 is large and comprable with that from In_2O_3. Moreover, the desorption peaks for Co_3O_4 occur in the relatively low temperature range of 100-300 °C and In_2O_3 also has a peak at 100-300 °C. In the case of ZnO and In_2O_3, the NO_2 desorption peaks appear at higher temperature of about 450 °C. This suggests that the NO_2 gas adsorbed at the YSZ/ZnO-SE and at the YSZ/In_2O_3-SE interfaces may promote the rate of the following cathodic reaction (1) of NO_2 at high temperatures:

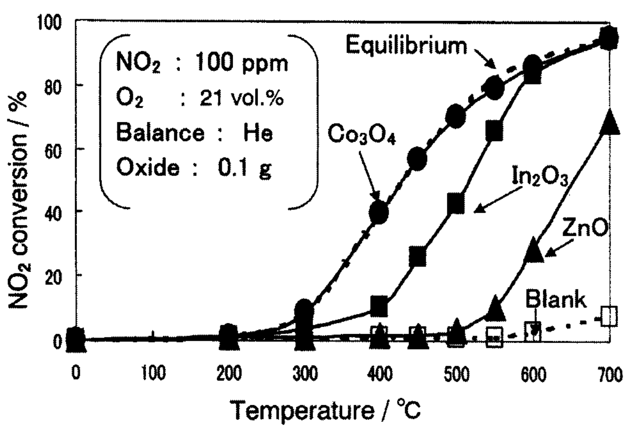

Fig. 7. Temperature dependence of NO_2 conversion to NO for the gas-phase decomposition reaction on the various oxides tested.

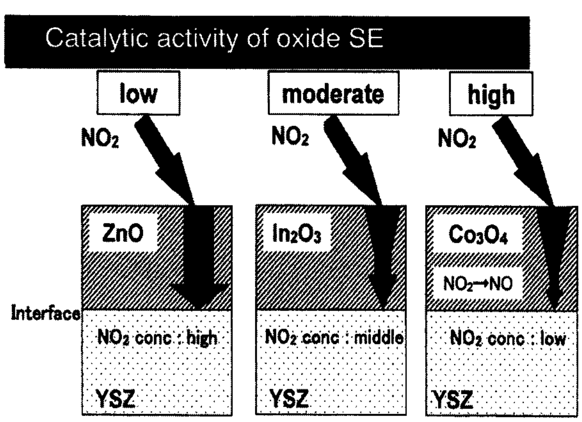

Fig. 9. Graphical explanation of the influence of catalytic activity of oxide SE on the actual concentration of NO_2 at the interface.

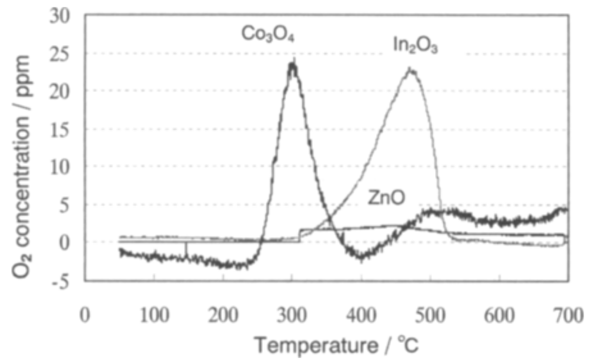

Fig. 10. TPD profiles of O_2 from ZnO, In_2O_3 and Co_3O_4 pow-- der samples.

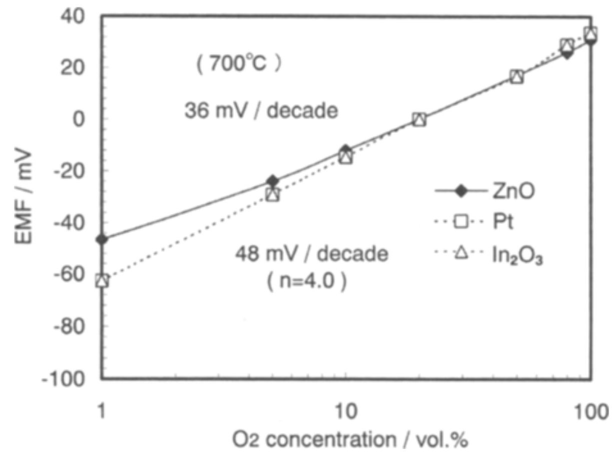

Fig. 11. Dependence of EMF on the logarithm of O_2 concentration for the YSZ devices using each of SEs at 700 °C.

$$NO_2 + 2e^- \rightarrow NO + O^{2-} \quad (1)$$

In spite of high desorption rate at relatively high temperature for In_2O_3, the NO_x sensitivity is still low for this oxide at 600 °C, as already gives in Fig. 3. Therefore, we examined the catalytic activity of these oxides tested for NO_2 decomposition reaction. Figure 7 shows the NO_2 conversion to NO due to the following non-electrochemical gas-phase reaction.

$$NO_2 \rightarrow NO + 1/2O_2 \quad (2)$$

In the gas mixture of 100 ppm NO_2, 21 vol.% O_2 and He balance, the NO_2 conversion on In_2O_3 is higher than that on ZnO at higher temperatures. Since NO, thermodynamically, dominates in the equilibrated NO_x gas mixture at temperatures above 500 °C [4], the conversion of NO_2 to NO is usually high when the effective catalysts are used. This indicates that the catalytic activity of ZnO is rather low, compared to those of other two oxides. Figure 8 shows that the catalytic activity for the oxides is roughly correlated to the NO_2 sensitivity obtained; the lower the catalytic activity of oxide, the higher the NO_2 sensitivity of the sensor. Figure 9 shows schematically the influence of catalytic activity of oxide on the actual concentration of NO_2 at the oxide/YSZ interface. If the catalytic activity of SE is reasonably high, most of NO_2 can be easily converted to NO accordingly to the gas-phase reaction (2) on the surface or in the bulk of oxide SE layer and thus it is rather difficult for NO_2 to arrive at the YSZ/SE interface (in the case of Co_3O_4). As a result, the NO_2 sensitivity is low for the device using such an SE. Conversely, if the catalytic activity of the SE is rather low, NO_2 can diffuse through the SE layer without serious decomposition to NO, and then almost all the NO_2 can reach the YSZ/SE interface, resulting in high NO_2 sensitivity (in the case of ZnO). When the catalytic activity is moderate, moderate NO_2 sensitivity is obtained (in the case of In_2O_3).

The investigation on O_2 desorption has revealed that the oxygen adsorbed on the oxide SE also plays a significant role in the sensing mechanism involving mixed potential. Figure 10 shows the TPD profiles for oxygen desorption from the oxides tested. The desorption peaks

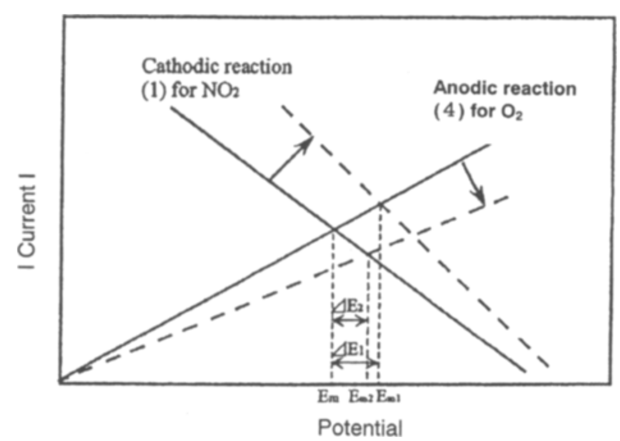

Fig. 12. Schematic polarization curves for the cathodic reaction (1) of NO_2 and anodic reaction (4) of O_2.

for both Co_3O_4 and In_2O_3 are significantly higher than that for ZnO. This suggests that the catalytic activity of the ZnO-SE for the electrochemical reaction involving O_2 is low.

To confirm this assumption, the oxygen sensing properties of the devices using ZnO and In_2O_3 were evaluated. For this purpose, the EMF values of the YSZ-based devices were measured when the oxagen concentration in the gas mixture (N_2+O_2) was changed from 1 to 100 vol.% at 700 °C. Figure 11 shows the Nernstian plots at 700 °C for the devices. As a comparison, the data for the sensor using the Pt-paste electrode were also given in this figure. The ZnO-SE provided smaller Nernstian slope (36 mV/decade) than the theoretical value (48 mV/decade, n = 4.0). On the other hand, In_2O_3-SE and Pt-SE gave the theoretical Nernstian slope. This indicates that the ZnO-SE is working as an irreversible oxygen electrode and then the catalytic activity of the ZnO-SE for the electrochemical reaction (3) of oxygen is low as expected. Thus, such a low electrochemical catalytic activity may also contribute to the high sensitivity to NO_2 of the present sensor at high temperatures.

$$O_2 + 4e^- = 2O^{2-} \tag{3}$$

Figure 12 shows the influence of electrochemical catalytic activity for both cathodic (1) and anodic (4) reactions on polarization curves, which schematically explains how the mixed potential works. The mixed po-

Table 2. Comparison between estimated mixed-potential values and observed EMF values for the YSZ-based device using ZnO-SE at 700 °C.

200 ppm NO		200 ppm NO_2	
E_{m1}	EMF	E_{m2}	EMF
– 15 mV	– 15 mV	+ 68 mV	+ 65 mV

$$2O^{2-} \rightarrow O_2 + 4e^- \tag{4}$$

tential (E_m) can be defined at the intersection of cathodic and anodic polarization curves, where the absolute values of cathodic and anodic currents are equal to each other. Both electrochemical reactions (1) and (4) proceed simultaneously at same reaction rate (same current density) at this potential E_m. If the catalytic activity for cathodic reaction (1) of NO_2 for oxide tested is high, the polarization curve for NO_2 shifts upward. Consequently, it changes the mixed potential to the direction of positive potential E_{m1} and increases the NO_2 sensitivity (ΔE_1). Alternatively, if the catalytic activity for anodic reaction of O_2 (4) is low, the anodic polarization curve for oxygen shifts downwards. The mixed potential, therefore, also changes to the direction of positive potential (E_{m2}) and gives the increase in NO_2 sensitivity (ΔE_2). For further verification of the mixed-potential model for YSZ-based NO_x sensor using the ZnO-SE, the polarization curves were measured for the ZnO-SE under exposure to both NO

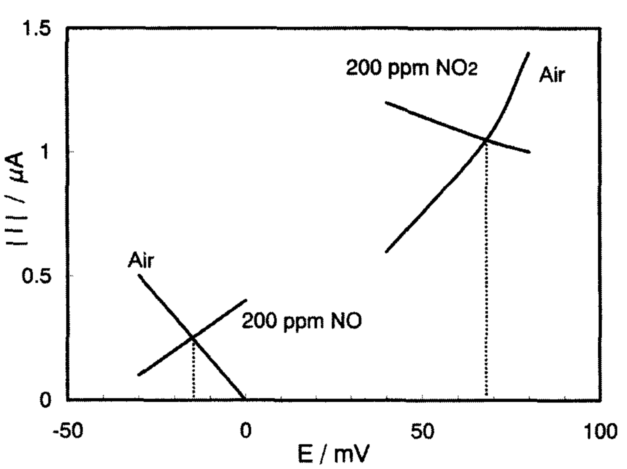

Fig. 13. Modified polarization curves of the YSZ sensor using ZnO-SE.

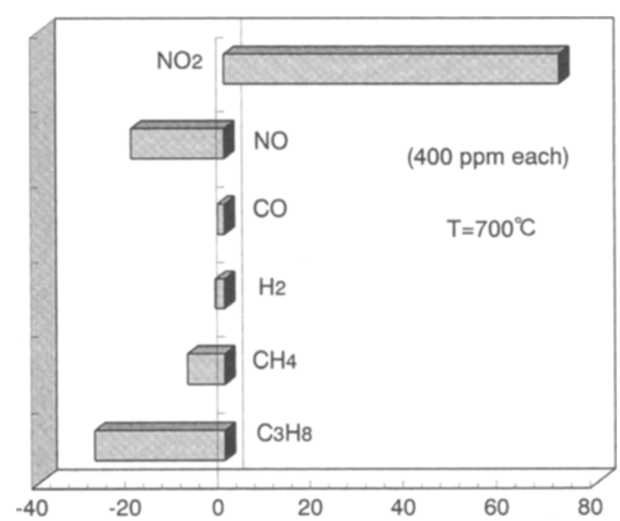

Fig. 14. EMF response (gas sensitivity) to various gases (400 ppm each) at 700 °C for the YSZ-based device attached with ZnO-SE.

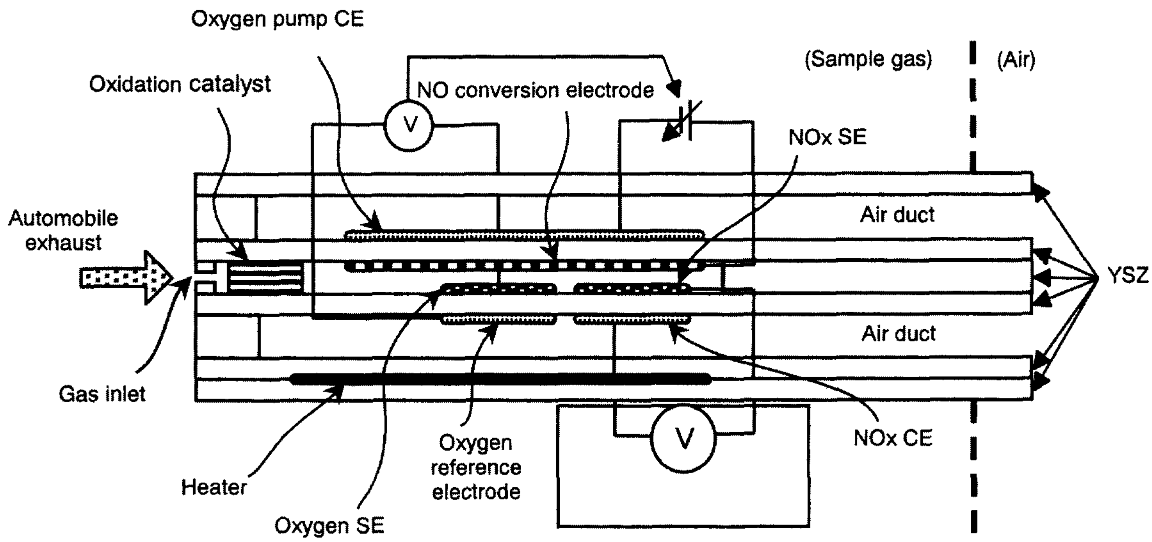

Fig. 15. Cross-sectional view of the laminated YSZ-based mixed-potential NO_x sensor.

and NO_2 (200 ppm each). The estimated mixed-potential values and the observed EMF values were in good agreement with each other (see Fig. 13 and Table 2), which confirms the mixed-potential model previously reported [5,6].

From the practical point of view, NO should be electrochemically oxidized forcibly to NO_2, since the response direction to NO of the present mixed-potential sensor is opposite to that to NO_2. As previously proposed [19], installation of an NO conversion electrode would allow the total NO_x content to be measured by the present NO_x sensing system using the ZnO-SE for detecting NO_2. In addition, the change in O_2 concentration in the sample gas can be compensated for by means of an O_2 sensing electrode (Pt) which is installed near the oxide SE. Furthermore, as shown in Fig. 14, the present YSZ-based NO_x sensor attached with the ZnO-SE have cross-sensitivities to combustible gases which usually exist in real car-exhausts. Thus, the combustible gases should be oxidized to CO_2 and H_2O before reaching the ZnO-SE, by using an oxidation catalyst. These functioning devices can be combined into a planar laminated-type NO_x device, as reported previously [19,20]. Therefore, in the laminated-type sensor, combustible gases can be first oxidized by the oxidation catalyst before they reach the SE and NO can be oxidized to NO_2 by the conversion electrode. Then, the change in O_2 concentration around the SE can be compensated for by the oxygen sensor. Consequently, the total NO_x content can be monitored without the interference of combustible gases as well as the variation in O_2 concentration.

4. Conclusions

The mixed-potential-type NO_x sensors using each of several single-oxide SEs were fabricated and their sensing properties were investigated in the temperature range of 600-700 °C. The YSZ-based device using the ZnO-SE gave the highest sensitivity to NO_x even at 700 °C among other single-oxide SEs tested here and reported to date. This suggests that ZnO is one of the promising candidate for SE of the practical NO_x sensor working at high temperature. Gas adsorption-desorption behavior, chemical and electrochemical catalytic activities, and other results suggest that the NO_2 sensitivity can be influenced by these factors in a complex manner. For the practical application, however, a laminated-type multi-component structure for the mixed-potential YSZ-based NO_x sensor should be used. The main advantage of this design is that the total NO_x content can be measured and the NO_x sensitivity can be protected from the influence of the co-existing combustible gases as well as from the deviation of oxygen concentration in exhaust gas.

5. Acknowledgements

This work was partially supported by a Grant from the Ministry of Education, Science, Sports and Culture of Japan.

6. References

[1] Official Journal of the European Communities, L 350, Vol. 41; European Directive 2000/25/EC, 22 May 2000.

[2] N. Miura, M. Nakatou and S. Zhuiykov, Sensors and Actuators B **93**, 221 (2003).

[3] N. Miura, G. Lu and N. Yamazoe, J. Elecrochem. Soc. **143**, L33 (1996).

[4] N. Miura, H. Kurosawa, M. Hasei, G. Lu and N. Yamazoe, Solid State Ionics **86-88**, 1069 (1996).

[5] N. Miura, G. Lu and N. Yamazoe, Sensors and Actuators B **52**, 169 (1998).

[6] G. Lu, N. Miura and N. Yamazoe, Sensors and Actuators B **65**, 125 (2000).

[7] S. Zhuiykov, T. Nakano, A. Kunimoto, N. Miura and N. Yamazoe, Electrochemistry Communications **3**, 97 (2001).

[8] S. Zhuiykov, M. Muta, T. Ono, A. Kunimoto, N. Yamazoe and N. Miura, Eletrochem. and Solid-State Letters **4**, H19 (2001).

[9] N. Miura, S. Zhuiykov, T. Ono, M. Hasei, N. Yamazoe, Sensors and Actuators B **83**, 222 (2002).

[10] S. Zhuiykov, T. Ono, N. Yamazoe and N. Miura, Solid State Ionics **152-153**, 801 (2002).

[11] N. Miura, T. Raisen, G. Lu and N. Yamazoe, J. Electrochem. Soc. **144**, L198 (1997).

[12] Y. Yan, N. Miura and N. Yamazoe, Chemistry Letters **1994**, 1753 (1994).

[13] N. Miura, T. Shiraishi, K. Shimanoe and N. Yamazoe, Electrochemistry Communications **2**, 77 (2000).

[14] Y. Shimizu and K. Maeda, Sensors and Actuators B **52**, 84 (1998).

[15] E.D. Bartolomeo, E. Traversa, M. Baroncini, V. Kotzeva and R.V. Kumar, J. European Ceramic Soc. **20**, 2691 (2000).

[16] W. Göpel, G. Reinhardt and M. Rösch, Solid State Ionics **136-1**37, 519 (2000).

[17] J.W. Yoon, M.L. Grilli, E.D. Bartolomeo, R. Polini and E. Traversa, Sensors and Actuators B **76**, 483 (2001).

[18] N.F. Szabo, H. Du, S.A. Akbar, A. Soliman and P.K. Dutta, Sensors and Actuators B **82**, 142 (2002).

[19] M. Hasei, T. Ono, Y. Gao, Y. Yan and A. Kunimoto, SAE Technical Paper Series, 2000-01-1203, p. 1-7.

[20] T. Ono, M. Hasei, A. Kunimoto, T. Yamamoto and A. Noda, JSAE Review **22**, 49 (2001).

Manuscript rec. Feb. 23, 2004; acc. Apr. 15, 2004.